International Journal of Medical Microbiology 309 (2019) 169–181

Contents lists available at ScienceDirect

International Journal of Medical Microbiology

journal homepage: www.elsevier.com/locate/ijmm

Biofilm development and computational screening for new putative inhibitors of a homolog of the regulatory protein BrpA in *Streptococcus dysgalactiae* subsp. *dysgalactiae*

Cinthia Alves-Barroco[a], Catarina Roma-Rodrigues[a], Natesan Balasubramanian[a,b], Marcia Aparecida Guimarães[c], Bernadete T. Ferreira-Carvalho[c], Jayaraman Muthukumaran[d], Daniela Nunes[e], Elvira Fortunato[e], Rodrigo Martins[e], Teresa Santos-Silva[d,*], Agnes M.S. Figueiredo[c,*], Alexandra R. Fernandes[a,*,1], Ilda Santos-Sanches[a,1,2]

[a] UCIBIO, Departamento de Ciências da Vida, Faculdade de Ciências e Tecnologia, Universidade Nova de Lisboa, Caparica, Portugal
[b] Department of Immunology, School of Biological Sciences, Madurai Kamaraj University, Madurai, 625021, India
[c] Instituto de Microbiologia Paulo de Góes, Universidade Federal do Rio de Janeiro, RJ, Brazil
[d] UCIBIO, Departamento de Química, Faculdade de Ciências e Tecnologia, Universidade Nova de Lisboa, Caparica, Portugal
[e] i3N/CENIMAT, Departamento de Ciência dos Materiais, Faculdade de Ciências e Tecnologia, Universidade Nova de Lisboa, Campus de Caparica, Caparica, Portugal

ARTICLE INFO

In memory of Ilda Santos-Sanches

Keywords:
Biofilm
Biofilm regulatory protein
BrpA inhibitors
Molecular docking
Streptococcus dysgalactiae subsp. *dysgalactiae*

ABSTRACT

Streptococcus dysgalactiae subsp. *dysgalactiae* (SDSD), a Lancefield group C streptococci (GCS), is a frequent cause of bovine mastitis. This highly prevalent disease is the costliest in dairy industry. Adherence and biofilm production are important factors in *streptoccocal* pathogenesis. We have previously described the adhesion and internalization of SDSD isolates in human cells and now we describe the biofilm production capability of this bacterium. In this work we integrated microbiology, imaging and computational methods to evaluate the biofilm production capability of SDSD isolates; to assess the presence of biofilm regulatory protein BrpA homolog in the biofilm producers; and to predict a structural model of BrpA-like protein and its binding to putative inhibitors. Our results show that SDSD isolates form biofilms on abiotic surface such as glass (hydrophilic) and polystyrene (hydrophobic), with the strongest biofilm formation observed in glass. This ability was mainly associated with a proteinaceous extracellular matrix, confirmed by the dispersion of the biofilms after proteinase K and trypsin treatment. The biofilm formation in SDSD isolates was also confirmed by confocal laser scanning microscopy (CLSM) and scanning electron microscopy (SEM). Under SEM observation, VSD16 isolate formed cell aggregates during biofilm growth while VSD9 and VSD10 formed smooth and filmy layers. We show that *brpA*-like gene is present and expressed in SDSD biofilm-producing isolates and its expression levels correlated with the biofilm production capability, being more expressed in the late exponential phase of planktonic growth compared to biofilm growth. Fisetin, a known biofilm inhibitor and a putative BrpA binding molecule, dramatically inhibited biofilm formation by the SDSD isolates but did not affect planktonic growth, at the tested concentrations. Homology modeling was used to predict the 3D structure of BrpA-like protein. Using high throughput virtual screening and molecular docking, we selected five ligand molecules with strong binding affinity to the hydrophobic cleft of the protein, making them potential inhibitor candidates of the SDSD BrpA-like protein. These results warrant further investigations for developing novel strategies for SDSD anti-biofilm therapy.

1. Introduction

Biofilms are heterogeneous structures composed of bacterial cells surrounded by a matrix and attached to solid surfaces (Olsen, 2015). During biofilm growth, bacteria are transferred from a free-swimming state (planktonic cells) to a multitude of bacterial cells enclosed by a self-produced polysaccharide matrix of hydrated extracellular polymeric substances, attached to biotic or abiotic surfaces (sessile cells)

* Corresponding authors.
E-mail addresses: tsss@fct.unl.pt (T. Santos-Silva), agnes@micro.ufrj.br (A.M.S. Figueiredo), ma.fernandes@fct.unl.pt (A.R. Fernandes).
[1] Co-last authors
[2] Deceased

https://doi.org/10.1016/j.ijmm.2019.02.001
Received 11 August 2018; Received in revised form 14 February 2019; Accepted 17 February 2019

(Flemming and Wingender, 2010). However, in some bacteria, such as *Staphylococcus aureus*, the biofilm matrix can be mostly composed by bacterial surface proteins and extracellular DNA (eDNA) (Toledo-arana et al., 2005). Biofilms can differentiate, to form mushroom- and tower-like structures surrounded by fluid filled channels (Olsen, 2015). Bacterial biofilms are ubiquitous in the environment and can be found on almost any hydrated non-shedding surface including rivers, stagnant pools, man-made and also biological materials (Garnett and Matthews, 2012). As a response to environmental changes such as pH, oxygen, carbon source and/or nutrient availability, cell density, and the presence of a solid surface, bacterial cells in biofilms interact with each other, resulting in the global coordination of their gene expression (Jefferson, 2004; Wen and Burne, 2002). Quorum sensing is the signaling network for cell-to-cell communication that regulates biofilms and other cellular processes (Galante et al., 2015).

Biofilm formation has been implicated in different types of bacterial infections in both humans and animals, making those infections difficult to eradicate with antimicrobials. This is the case, for example, of orthopedic and cardiac implant-associated infections, cystic fibrosis, urinary tract infections, osteoarticular infections and periodontal diseases (Olsen, 2015). Many persistent and chronic bacterial infections are now thought to be linked to biofilm formation, and over 60% of all bacterial infections have been estimated to involve biofilms (Kvist et al., 2008; Reid et al., 2009). Biofilm-associated infections are particularly problematic because bacteria sessile cells tolerate host defense mechanisms, antibiotics, biocides, and hydrodynamic shear forces far better than the corresponding planktonic ones (Dürig et al., 2010; Rosini and Margarit, 2015). Therefore, biofilms are clinically important not only because they form a defensive barrier against other potential pathogens (in case of the host microbiota), but they also generate a break line between minor and debilitating infectious diseases. Indeed, biofilms can promote horizontal spread of resistance determinants (Savage et al., 2013).

Streptococcus can form biofilms on natural or abiotic surfaces such as glass (hydrophilic) or polystyrene (hydrophobic) (Marks et al., 2014a,b; Oliver-Kozup et al., 2011; Silva et al., 2014). Studies in *Streptococcus mutans* showed that several genes are required for biofilm development (Bitoun et al., 2014; Shemesh et al., 2007a). Several studies reported that the expression of genes responsible for biofilm formation is dependent on environmental conditions (Li and Burne, 2001; Shemesh et al., 2007a) and genetically regulated (Lee et al., 2004). In 2007, Shemesh et al described in *Streptococcus mutans* the presence of the paralogues *brpA* and *brpB*, encoding the biofilm regulatory proteins A and B (BrpA and BrpB, respectively) which are members of the LytR/CpsA/Psr– LCP family (Shemesh et al., 2007a). The LCP family of proteins, important for the bacterial adaptation in different environments, has been found in the genome of both pathogenic and non-pathogenic bacteria (Chatfield et al., 2005). LCP proteins have an important role in cell-wall biogenesis and structural maintenance, by regulating autolysin. In addition, these proteins have been implicated in biofilm development and bacterial adhesion to host cells (Bitoun et al., 2014; Shemesh et al., 2007b). Considering the importance of biofilm development in a plethora of infectious diseases (Del Pozo, 2018), including bovine mastitis by *Staphylococcus aureus* (Ghinet et al., 2017), and the fact that *Streptococcus dysgalactiae* subsp. *dysgalactiae* (SDSD) is an important mediator of this bovine disease and also capable to infect human cells (Alves-Barroco et al., 2018; Jordal et al., 2015; Koh et al., 2009; Park et al., 2012; Roma-Rodrigues et al., 2015), characterizing biofilm formation by SDSD is a major step to mitigate infection. Thus, the aim of the present study was to evaluate and characterize biofilm production by SDSD isolates and to assess the presence of the *brpA*-like gene (*lytR*-like). Using *in silico* methods, we predicted the 3D-homology model of the cytoplasmic domain of BrpA homolog protein of SDSD and combined high throughput virtual screening-molecular docking to identify potential inhibitors of this protein.

2. Materials and methods

2.1. Ethical statement

The study design followed the international (Directive 2010/63/EU of the European parliament, on the protection of animals used for scientific purposes) and national (Decreto-Lei nº 113/2013) welfare regulations and guidelines (ARRIVE). Sample collection was previously approved by the Portuguese "Direção Geral de Alimentação e Veterinária (DGAV)" (authorization document 0421/000/000/2013). In addition, two authors have a level C FELASA certification (Federation of European Laboratory Animal Science Associations).

2.2. Bacterial collection and identification

A total of 18 alpha-hemolytic SDSD isolates from Portuguese animals diagnosed with subclinical and clinical mastitis were used in the present study. Detailed information regarding these field isolates, including identification and molecular typing data, was previously described (Rato et al., 2010). A alpha-hemolytic SDSD isolate from Canada (GCS-Mo), associated with bovine cellulitis and Toxic Shock-Like Syndrome, and another from Singapore, (GCS-Si) responsible for an ascending upper limb cellulitis in a woman that was pricked by the fins and scales of a raw fish, were also included in this study (Rato et al., 2011). Additionally, two Portuguese *S. dysgalactiae* subsp. *equisimilis* (SDSE) COI 289 and HSM 53 isolates, and one *S. pyogenes* GAP58 (Alves-Barroco et al., 2018) isolate, were also included in this study for comparative analysis. The SDSE isolates were already identified by our group as weak and strong biofilm producers on glass and polystyrene and hence were used as controls (Genteluci et al., 2015).

2.3. Media, bacterial growth and storage condition

Colombia agar supplemented with 5% (v/v) sheep blood (Probiologica, Belas, Portugal) was used for colony isolation. The bacteria were grown in Todd-Hewitt broth (BBL, Cockeysville, Md., USA) supplemented with 1% (w/v) of yeast extract (Oxoid, Basingstoke, United Kingdom) and incubated at 37 °C for 14–16 h. The late exponential phase culture was mixed with 20% (v/v) sterilized glycerol and were kept and maintained at −80 °C.

2.4. 16S rRNA amplification and species identification

The 16S rRNA gene was amplified using the forward 5′ AGAGTTT GATCCTGGCTC' 3 and reverse 5′ GGTTACCTTGTTACGACTT' 3 primers (Rato et al., 2011). PCR conditions were 95 °C for 5 min followed by 35 cycles of 95 °C for 1 min, 55 °C for 1 min, 72 °C for 2 min and a final extension step at 72 °C for 10 min, and amplification was performed in a thermocycler (Biometra, Göttingen, Germany). The 1476 bp PCR product was analysed in 1% (w/v) agarose gel. The PCR products were sequenced with specific primers, and the DNA sequences were analyzed using *BioEdit sequence alignment* tool and compared with the sequences deposited in the National Center for Biotechnology Information (NCBI)-GenBank database using the *BLAST alignment* tool (www.ncbi.nlm.nih.gov/BLAST).

2.5. Biofilm formation assay on glass

Biofilm production on glass surfaces was carried as previously described (Ferreira et al., 2012; Genteluci et al., 2015). SDSD, SDSE and GAP58 isolates were streaked on a blood agar plate and incubated at 37 °C for 18 h in a 5% (v/v) CO_2 incubator. About 5–10 colonies were transferred to 4 mL of Trypticase Soy Broth (TSB) supplemented with 0.5% (w/v) glucose and incubated overnight at 37 °C in a water bath without agitation. Culture growth was followed by measuring the optical density (OD) at 570 nm (OD_{570}). 100 µL of bacterial culture

(OD_{570} = 0.6) was transferred to a test tube containing 3.9 mL of TSB supplemented with 0.5% (w/v) glucose and incubated in a horizontal position for 20 h at 37 °C. The supernatant was carefully removed and washed with sterile saline solution (0.85% (w/v) NaCl) by manually rotating the tube. The test tubes were incubated in an oven at 65 °C for 1 h or at 45 °C for 3 h for the attachment of biofilm. The biofilm formation capability of each strain was classified by visual inspection as weak (+); moderate (++); and strong (+++). Biofilms were resuspended in 4 mL of saline solution. Then, the OD at 600 nm (OD_{600}) was measured (saline solution as blank) and used to rate biofilm formation: $OD_{600} \leq 0.099$, no formation; OD_{600} between 0.1–0.299, weak; OD_{600} between 0.3–0.599, moderate; $OD_{600} > 0.600$, strong (Ferreira et al., 2012).

2.6. Biofilm formation assay on polystyrene

Biofilm production on polystyrene surfaces was carried as previously described (Ferreira et al., 2012). Briefly, 100 µl of bacterial culture (OD_{570} = 0.6) was added to 100 µl of TSB broth supplemented with 0.5% (w/v) glucose in a 96 well plate and mixed by pipetting. A 200 µl of TSB broth supplemented with 0.5% (w/v) of glucose was used as control. The 96 well plate was sealed and incubated for 20 h at 37 °C. The OD_{570} was measured in an ELISA plate reader (Bio Rad, California, USA). The supernatant was carefully removed, and each well was washed twice with sterile saline solution (0.85% w/v) to remove non-adherent bacteria and dried at 65 °C for 1 h. The biofilm was stained with crystal violet 1% (w/v) for 1 min. The wells were washed again gently with sterile distilled water 3 or 4 times (until the control-wells dye was completely removed). The OD_{570} of the stained biofilm was directly measured in the plate reader. Interpretation of biofilm formation was performed according to the criteria previously described (Stepanović et al., 2007) and the isolates were therefore categorized as follows: non producer: $OD \leq OD_{ctrl}$, (all strains which OD values were below 0.060); weak producer: $OD_{ctrl} < OD \leq 2 \times OD_{ctrl}$, (all strains which OD values were above 0.060 and below 0.120); moderate producer: $2 \times OD_{ctrl} < OD \leq 4 \times OD_{ctrl}$ (all strains which OD values were above 0.120 and below 0.240). strong producer: $OD > 4 \times OD_{ctrl}$ (all strains which OD values were above 0.240).

2.7. Characterization of extracellular polymeric matrix by Congo Red Agar (CRA) binding assay

A modification of a previously described Congo Red Agar (CRA) binding assay was used to detect extracellular polysaccharides (Rollefson et al., 2011). The strains were grown in Todd Hewitt broth (18 h/37 °C). Cells were harvested by centrifugation (9072 × *g* for 10 min), washed twice with phosphate buffered saline (PBS, containing 137 mM NaCl; 2.7 mM KCl;10 mM Na_2HPO_4; 2 mM KH_2PO_4, pH 7.4) and the density of the suspension was adjusted to an optical density (OD_{600}) of 0.5. Cells were cultured in Todd Hewitt Agar supplemented with different sugars (glucose, sucrose or lactose), at different concentrations (1, 2 and 5% (w/v)), and 0.08% (v/v) Congo Red (Sigma-Aldrich Missouri, USA). All plates were incubated for 24 h at 37 °C in aerobic atmosphere with 5% (v/v) CO_2. The presence of polysaccharides was indicated by black colonies with a dry crystalline consistency. Weak or non-polysaccharide producing colonies remained red. The darkening of the colonies with the absence of a dry crystalline colonial morphology indicated an indeterminate result. The *Staphylococcus aureus* ATCC 25923 was used as a positive control.

2.8. Enzymatic treatment of the biofilm matrix

Bacteria were grown in a 4 mL of TSB supplemented with 0.5% (w/v) of glucose, incubated overnight at 37 °C in a water bath without agitation. The culture was grown until an OD_{570} of 0.6, and 50 µL was transferred to 2 mL of TSB medium supplemented with 0.5% (w/v) glucose containing: i) pronase or protease (0.75 U/mL), ii) trypsin (55 U/mL), iii) proteinase K (30 U/mL; (Ferreira et al., 2012)), iv) DNase I (280 U/mL) or v) sodium metaperiodate (10 mM). After an incubation for 20 h at 37 °C, the supernatant was removed, and the tube washed with 2 mL of distilled water. The biofilm formation was classified by visual inspection as stated above and quantified by measuring the OD_{600} after resuspension in 2 mL of saline solution (0.85% (w/v) NaCl, (Genteluci et al., 2015).

3. Analysis of the biofilm structure using fluorescence microscopy, confocal laser scanning microscopy (CLSM) and scanning electron microscopy (SEM)

The structure of the biofilm produced by three SDSD isolates - VSD9, VSD10 and VSD16 - was analyzed by fluorescence microscopy, CLSM and SEM.

For fluorescence microscopy studies, SDSD isolates were grown over a cover glass as previously described (Roma-Rodrigues et al., 2015). The media containing the non-adherent cells was removed and the biofilms were gently washed (3 times) with PBS and stained with the LIVE/DEAD reagent (0.25 µg/mL propidium iodide (PI) and 20 µM Carboxy fluorescein succinimidyl ester (CFSE) in PBS; Life Technologies, Carlsbad, CA, USA) for 30 min. After 3 washes with PBS, the cover glass was placed in a microscope slide on a drop of ProLong Diamond antifade mountant (LifeTechnologies). Biofilms were imaged using a fluorescence microscope Zeiss Axioplan 2 Imaging Microscope coupled with a Nikon DXM1200 F digital camera (software ZEN Blue edition, 2011). CFSE was used to stain live cells (excitation and fluorescence emission at 492 and 517 nm, respectively); PI was used to stain dead cells (maximal excitation and fluorescence emission at 565 and 617 nm, respectively). A microscope objective of 40× magnification plus ocular lenses of 10x magnification (total magnification of 400×) were used. The amplification used for collecting the images is described in the respective Figure caption.

For CLSM, biofilms were produced and fixed as described above for fluorescence microscopy. Subsequently, the cells were treated with Triton X-100 at 0.1% (v/v) (Sigma), washed with PBS and stained with Hoechst 33,258 (0.2 µg/mL, Life Technologies, Carlsbad, CA, USA) for 1 h at 37 °C in the dark. Samples were washed 3 times with PBS and the cover glass containing the biofilm was placed on top of a drop of ProLong Diamond antifade mountant (Life Technologies, California, USA) in a microscope slide. To determine the biofilm thickness, 10 different regions per microscope slide were analysed using a fluorescence confocal microscope (CLSM, Carl Zeiss, LSM 700) and the top and bottom layers of the thicker region of the biofilm and the maximum biofilm height measured using the software ZEN Black, 2011. Three measures in each microscopic field were used for analysing the thickness of the biofilm.

SEM procedure followed the protocol described by Pluk et al. (2009) with some little modifications. A commercial indium tin oxide (ITO) glasses were gently washed with 70% (v/v) ethanol, followed by sterile water and then placed in a sterile Petri plate with a lid. 100 µL of bacterial culture (OD = 0.6) was added to a 1.9 ml of TSB medium with glucose (0.5%) and added to the ITO glass. The glass plates were incubated for 20 h at 37 °C. The media was carefully removed, washed with sterile saline solution (NaCl 0.85%) to remove planktonic cells and dried for 1 h at 37 °C. The ITO glasses with biofilms were frozen in liquid nitrogen and subsequently dried in a freeze-dryer (TLMCSP-80, Thermoline L + M, Northgate, QLD, Australia) at −30 °C under vacuum for 10 min (Crang and Klomparens, 1988; Dykstra and Reuss, 2003). The samples were warmed to room temperature before use. SEM observations were carried out using a Carl Zeiss AURIGA CrossBeam (FIB-SEM) workstation, equipped for EDS and EBSD measurements.

4. Inhibition of biofilms by fisetin

Fisetin (Sigma-Aldrich Missouri, USA) was used to inhibit biofilm development as previously described (Dürig et al., 2010). SDSD isolates VSD1, VSD9 and VSD16 were used for these inhibition studies. About 5 colonies were transferred to 4 mL of TSB supplemented with glucose 0.5% (w/v) and incubated overnight at 37 °C. Culture growth was followed by measuring the OD_{570}. 100 µL of bacterial culture (OD_{570} = 0.6) was transferred to a test tube containing 3.9 mL of TSB supplemented with 0.5% (w/v) glucose and three different concentrations of fisetin -32 µg/mL, 64 µg/mL and 128 µg/mL. The tubes were incubated in a horizontal position for 20 h at 37 °C. The supernatant was carefully removed, washed with saline solution (0.85% (w/v) NaCl) by manually rotating the tube. The tubes were incubated in an oven at 65 °C for 1 h for biofilm attachment. Biofilms were resuspended in 4 mL of saline solution and the OD_{600} measured.

5. Genomic DNA preparation

Genomic DNA was obtained according to (Seppalla et al., 1998) with few modifications. Briefly bacterial cells were grown in 4 mL of Todd-Hewitt broth (BBL, Cockeysville, Md.) supplemented with 1% (w/v) of yeast extract (Oxoid, Basingstoke, United Kingdom) at 37 °C for 16–18 h. The culture was centrifuged at 11,269 *g* for 3 min and the pellet resuspended in 500 µl of 10 mM Tris − HCl (pH 8.5). Cell lysis was obtained by incubating (2 h at 37 °C) the bacterial suspension with 40 µL of lysozyme (0.8 mg/mL final concentration) and 11 µL of mutanolysin (110 U/mL or 0.5 mg/mL final concentration). The lysate was centrifuged at 13,552 × *g* for 10 min at 4 °C. The DNA was extracted once with 1 mL phenol:chloroform (1:1). The water phase was then collected, and the DNA precipitated by overnight incubation at − 20 °C using 2 volumes of cold ethanol (P.A.) containing 0.3 M sodium acetate (pH 5.2). The pellets were washed with 70% (v/v) ethanol and dried in an oven at 50 °C for 20 min. The DNA was dissolved in 50 µL of milli-Q water, and stored at − 20 °C.

5.1. Polymerase Chain Reaction (PCR) amplification of brpA-like gene

The genome sequence of SDSE strain of Lancefield's group A antigen AC-2713 (Genebank accession number NC_019042) was used to design specific primers for *brpA*-like (*lytR*-like) gene: *lytR*-For 5′-ATGAAAAT TGGAAAAAAAATA-3′; *lytR*-Rev 5′-TTAAGGAAGAGAGGTGGTTGTA-3′ (Invitrogen). The PCR reactions were performed in a thermocycler (Biometra, Göttingen, Germany) in a final volume of 25 µL containing: 1 µL of bacterial genomic DNA (0.01 µg), PCR buffer, 2.5 mM of $MgCl_2$, 0.4 mM dNTPs, 1U Taq polymerase (NZYTech, Lisbon, Portugal) and 1 µM of each primer (Invitrogen). The PCR conditions consisted of an initial denaturation cycle (95 °C for 5 min) followed by 35 cycles of denaturation (95 °C for 30 s), annealing (42 °C for 30 s), and extension (72 °C for 80 s). A final extension at 72 °C for 7 min was also performed. Milli-Q water was used as a negative control in each PCR reaction.

The PCR products were analyzed by electrophoresis on 1% (w/v) agarose gel mixed with 5 µL (5 µg/100 mL) of Green Safe Premium (NZYTech). The PCR product (5 µL) was mixed with NzyDNA loading dye (1 µL, NZYTech) and loaded into the agarose slot (Sigma-Aldrich Missouri, USA). TAE buffer (Tris-Acetate-EDTA, pH 8.0) was used as a running buffer. DNA was visualized by UV light and photographed with a digital capture system (BioRad, California, USA). The 100 bp molecular weight marker Ladder III (NZYTech) was used to estimate DNA fragment size.

6. DNA sequencing analysis

The PCR products of *brpA*-like gene were purified using the Wizard PCR Preps DNA Purification System (Promega, Madison, USA). Sequencing was performed by STAB-Vida (Lisbon, Portugal) using specific primers (Table 1). The DNA sequence was analyzed by CLC Genomics Workbench 7.0.4 alignment program.

Table 1
Primer sequences used to amplify *brpA*-like gene.

Primer name	Primer sequence (5′→3′)	Product size (bp)
P1 F	TAA ATC AAA AGA TGG AGA TG	512
P1 R	GTG ATA TTC AAA AGG TCC TG	
P2 F	TGA AGC TAA GTT GAA TGC TGC	534
P2 R	GAA CCA CCA TCA GAC AAG GT	
P3 F	ATT AGG TTA TCG GGA TGC CCT C	544
P3 R	AGA ATG CTA AGC TGG TTG TTT	

6.1. brpA-like expression analysis

6.1.1. Total RNA preparation and cDNA synthesis

All isolates were grown in Todd-Hewitt broth (Oxoid Limited, Basingstoke, England) supplemented with 1% (w/v) of yeast extract (BD, Franklin Lakes, NJ, USA) at 37 °C until the mid-exponential phase of growth (OD_{600} of 0.5-0.6). RNA was extracted using NucleoSpin RNAII kit (Macherey-Nagel, Dueren, Germany) according to the manufacturer's instructions, followed by the addition of 2 U/µl of DNase I (Applied Biosystems/Ambion, California, USA). RNA was quantified in a Nanodrop Spectrophotometer (Thermo Scientific, Massachusetts, USA), integrity confirmed by gel electrophoresis [1% (w/v) agarose], and images were captured using the Gel Doc XR system and Quantity One 1-D analysis software (Bio-Rad). The cDNA was synthesized from 100 ng of total RNA using SuperScript first strand synthesis system (Invitrogen) according to manufacturer's instructions.

6.1.2. Reverse transcription - PCR (RT-PCR)

The *brpA*-like gene expression was analyzed using cDNA as a template and the same primers and conditions described above for PCR amplification. 16S RNA gene was used as an endogenous control. The PCR products were analyzed by gel electrophoresis [1% (w/v) agarose]. A molecular weight marker Ladder III (NZYTech) was used to estimate DNA fragment size.

6.1.3. Real-time quantitative PCR (RT-qPCR)

The quantitative analysis of *brpA*-like gene expression of the three SDSD isolates - VSD9, VSD10 and VSD16 - was carried out by RT-qPCR. For obtaining total RNA, cells were harvested after 20 h of incubation (biofilm forming conditions); during late exponential phase of planktonic growth (OD_{600} of 1.2–1.4) and in the stationary phase planktonic growth (20 h of incubation). All isolates were grown in TSB supplemented with 0.5% (w/v) and incubated under the same conditions used for analysis of biofilm formation on glass. Extraction of total RNA and cDNA synthesis was performed as described above. The RT-qPCR reaction mixture (20 µL) contained NZY qPCR Green Master Mix (NZYTech, Lisbon, Portugal), 1 µL cDNA, and 0.5 µM of the P2F and P2R primers described in Table 1. PCR conditions included an initial denaturation at 95 °C for 10 min, followed by 30 cycles of amplification consisting of denaturation at 95 °C for 15 s, and annealing at 58 °C for 30 s and extension at 60 °C for 45 s. All primer pairs were checked for primer-dimer formation by using the dissociation curve analysis. The critical Ct was defined as the cycle in which fluorescence becomes detectable above the background fluorescence. The expression levels of *brpA*-like gene were normalized using the 16S rRNA gene of SDSD as an internal standard. There was no significant difference in the expression of the 16S rRNA gene under the various conditions nor in the various samples tested. Each assay was performed with at least three independent RNA samples (and using technical duplicates). Student's *t*-test was used to calculate the significance of the difference between the mean expression of *brpA* gene in biofilm growth compared to planktonic growth (late exponential phase and stationary phase). A P value

of < 0.05 was considered significant.

6.1.4. Sequence analysis of the BrpA homolog protein using Bioinformatics tools

The *brpA*-like gene sequence of SDSD strain VSD9 (NCBI Accession Number: AIZ65938) was translated into the BrpA homolog protein by NCBI ORF Finder (http://www.ncbi.nlm.nih.gov/projects/gorf/orfig.cgi) and subjected to protein sequence analysis (ExPASy Proteomics Server; www.expasy.org/tools) (Gasteiger et al., 2005).The ProtParam web server (Gasteiger et al., 2005) was used to compute the physicochemical properties such as: i) amino acid composition, ii) molecular weight (MW), iii) isoelectric point (pI), iv) instability index (II), v) aliphatic index (AI) and vi) extinction coefficient (EC). Functional domains present in the protein sequence were identified by Motif search (http://www.genome.jp/tools/motif/). The sub cellular localization of the protein was predicted using PSort server (http://psort.hgc.jp/) (Gardy et al., 2003) and the presence of *N*-terminal signal peptide in the protein sequence were identified through TOPCONS server (http://topcons.cbr.su.se/) (Tsirigos et al., 2015).

6.1.5. Protein structure prediction and identification of putative inhibitors for BrpA homolog

The protein sequence of the BrpA homolog was submitted to Protein BLAST server (http://blast.ncbi.nlm.nih.gov/Blast.cgi?PAGE=Proteins) (Camacho et al., 2009) against Protein Data Bank (http://www.rcsb.org/pdb/home/home.do) (Berman et al., 2000) to identify suitable structural templates. Subsequently, the ModWeb server (https://modbase.compbio.ucsf.edu/modweb/) (Pieper et al., 2011) was used to predict the three-dimensional model of the homolog protein and the structural quality of the *in silico* generated model was investigated by RamPage (http://mordred.bioc.cam.ac.uk/rapper/rampage.php) server (Lovell et al., 2003) for analysis of the Ramachandran plot. Finally, the DrugDiscovery@TACC web portal (https://drugdiscovery.tacc.utexas.edu/) was used to perform the High Throughput Virtual Screening (HTVS) analysis of BrpA homolog against a Zinc Natural compound database (http://zinc.docking.org/) (Irwin and Shoichet, 2005) using Auto Dock Vina (Trott and Olson, 2010). Based on the literature (Dürig et al., 2010), we used ellagic acid and fisetin molecules as a reference and standard for the comparison of docking results with putative inhibitors. Binding mode, binding orientation, interacting residues and intermolecular interactions were carried out using LigPlus (Laskowski and Swindells, 2011) and figures were prepared using PyMOL (http://pymol.org/) (Rother, 2005).

6.1.6. Statistical analysis

All data were expressed as mean ± SEM from at least three independent experiments. GraphPad Prism version 7.0 was used for statistical analysis. The statistical significance was determined for each data set using the Student's *t* test and statistical significance was considered when $p < 0.05$.

7. Results

7.1. Biofilm development assay on glass surfaces

The ability of the 20 SDSD isolates to develop biofilms on glass surfaces was evaluated after 20 h of growth (under glucose (0.5% (w/v) induction) and compared with SDSE producer and non-producer control strains previously described by us (Genteluci et al., 2015). Portuguese SDSE COI 289 and HSM 53 and *S. pyogenes* GAP58 isolates analysis was also carried out for comparison. All 20 SDSD isolates and the SDSE COI 289 accumulate heavy amounts of biofilms on glass (Fig. 1A, S1 Fig and S1 Table Supplementary file). The *S. pyogenes* GAP58 and SDSE HSM53, were not capable of producing biofilms (Fig. 1A).

7.2. Biofilm formation assay on polystyrene

The ability of all the isolates to form biofilms on a polystyrene surface was also evaluated. Among the tested isolates, SDSD VSD2 and VSD6 produced high levels of biofilms; SDSD VSD5, VSD9, VSD15, GCS-SI and GCS-MO were classified as weak producers; and the remaining 13 SDSD isolates were not able to develop biofilm in polystyrene (Fig. 1B). SDSE HSM53 and COI 289 produced high levels of biofilms, whereas the *S. pyogenes* GAP58 isolate did not produce biofilm on this surface (Fig. 1B).

7.3. Characterization of biofilm composition matrix

The biofilm matrix was initially evaluated using CRA Method. After 24 h-incubation, all SDSD isolates were identified as non-producers of extracellular polysaccharide. The biofilm composition was also evaluated by treatment with proteinase K, trypsin, DNase, and sodium metaperiodate. Only proteinase K and trypsin caused a drastic dispersion of the biofilm accumulated, suggesting that the biofilm produced by SDSD isolates on glass surfaces was mainly associated with a proteinaceous extracellular matrix (Supplementary file, S1 Table).

7.4. SDSD biofilm analysis by fluorescence microscopy, confocal laser scanning microscopy (CLSM) and scanning electron microscopy (SEM)

Fluorescence microscopy, CLSM and SEM were used to get further insights into the biofilm structure. SEM has been previously used for studying different biofilm morphologies and structures (Gomes and Mergulhão, 2017; Kostakioti et al., 2013; Parnasa et al., 2016). The results obtained suggest that the biofilms produced by the SDSD isolates VSD9 and VSD10 are different from the biofilm produced by VSD16 isolate (Figs. 2, 3 and 4). Fluorescence microscopy also shows a higher number of dead cells in the biofilm produced by VSD16 (Fig. 2). Indeed, CLSM results indicate that VSD9 and VSD10 biofilms could cover 90% of the glass (Fig. 3A and B), with thickness ranging between 9–12 µm and 8–14 µm, respectively. Furthermore, VSD16 isolate forms several coccoid bacterial aggregates on glass that are denser in the middle, with a thickness of 15 µm (Fig. 3C).

Combining the results of SEM and CLSM images, biofilms produced by VSD9 and VSD10 isolates show a similar structure. However, VSD16 biofilm shows the presence of a massive amount of mucus-like extracellular material masking the cell surface (Fig. 4). It is possible that this mucous matrix might be formed by extracellular DNA (eDNA) liberated from VSD16 dead cells (visualized with CLSM) or by complexes of eDNA and bacterial proteins, since this matrix was also disrupted by proteinase (Fig. 2). Biofilms atomic composition is rich in oxygen and carbon (Fig. 4).

7.5. Inhibition of biofilm formation by Fisetin

The previous demonstration that ellagic acid and fisetin are able to impair biofilm production by Gram-positive bacteria, with a stronger effect for fisetin (Dürig et al., 2010), led us to analyze the effect of this molecule on the biofilm production by SDSD. We found that this compound shows an important inhibitory effect on biofilm developed by VSD1, VSD9 and VSD16 SDSD isolates in a concentration independent manner (Fig. 5), and that, at the tested concentrations, it is non-toxic for planktonic growth: no difference in the OD value was observed between the growth of control cells (planktonic) and that of the different concentrations of compound. However, macroscopic cell aggregates were formed in the presence of fisetin (32 µg/mL) (Supplementary file, S2 Fig).

7.6. Detection of brpA-like gene in SDSD isolates by PCR

Because of the importance of BrpA (LytR) proteins in bacterial

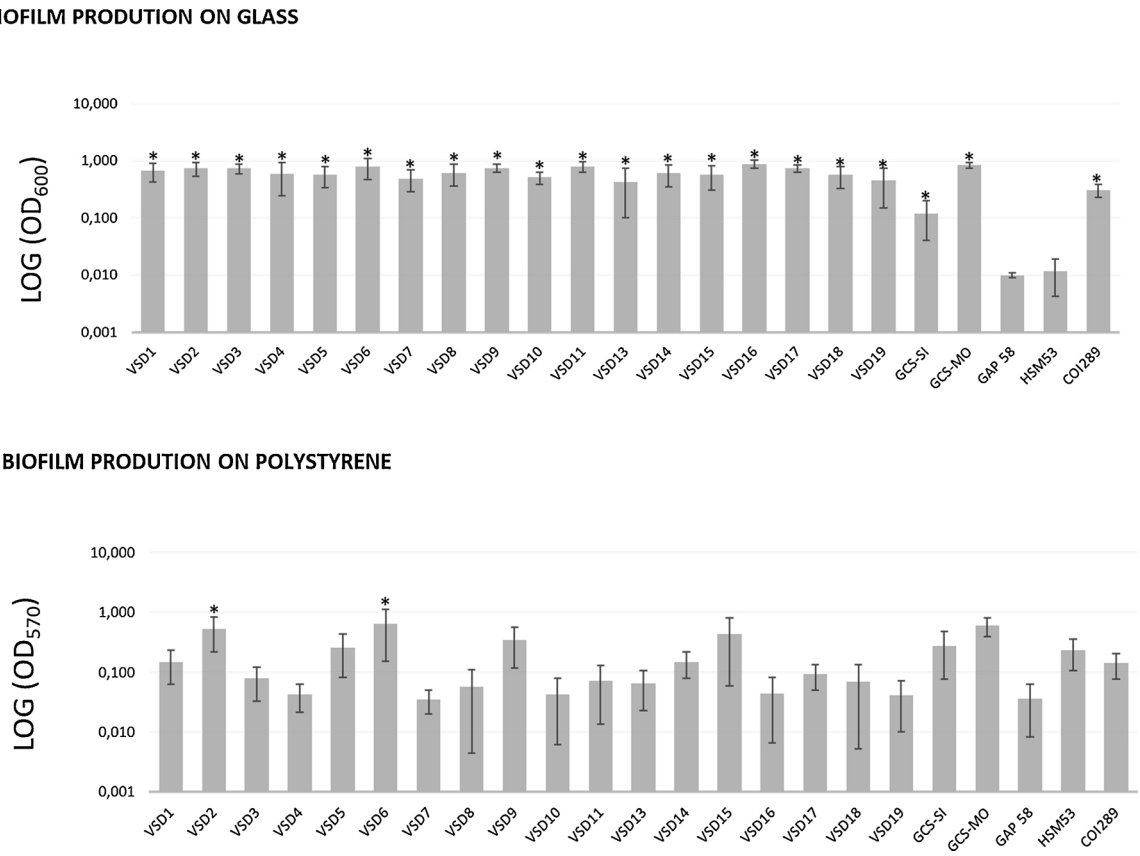

Fig. 1. Biofilm development on glass (A) and polystyrene (B) surfaces by *Streptococcus dysgalactiae* subsp. *dysgalactiae* (SDSD). **VSD1-11 and VSD13-19:** SDSD isolates obtained from clinical and subclinical mastitis in cattle. **GCS-SI:** SDSD isolate associated with an invasive infection of a human host in contact with raw fish.**GCS-MO:** SDSD associated with bovine cellulitis and toxic shock like syndrome. **HSM53:** SDSE from human blood. **COI289:** SDSE from human oropharynx. **GAP58:** *S. pyogenes* from human blood. Represented values are the mean value with SEM. *p-value < 0.05 for results obtained for VSD strains relative to the SDSE negative control strain (Genteluci et al., 2015).

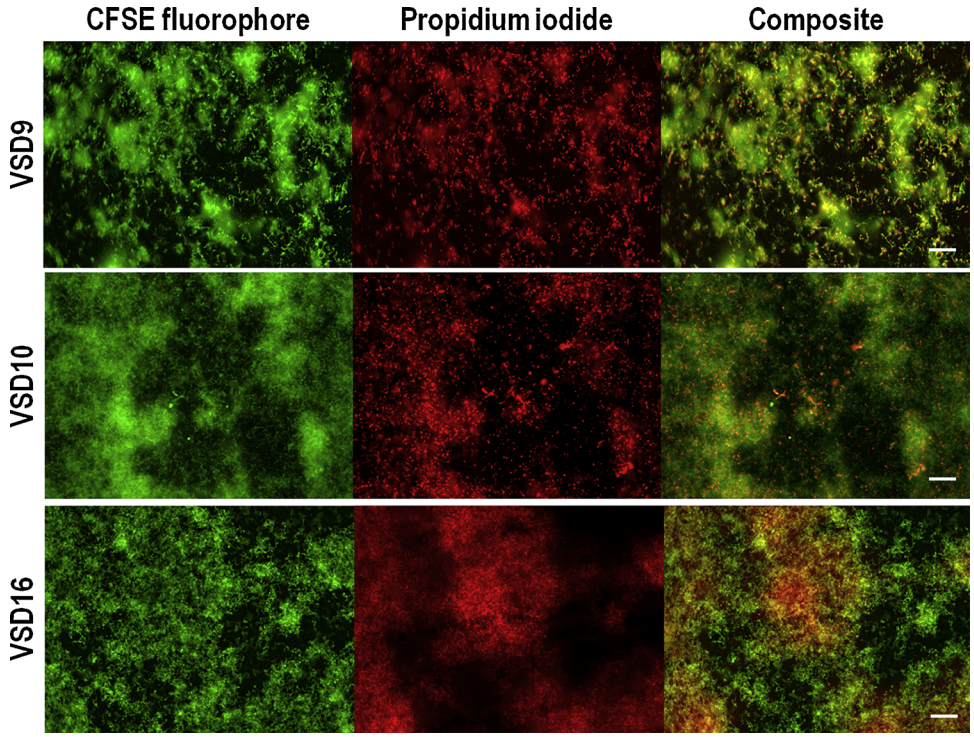

Fig. 2. LIVE/DEAD fluorescence imaging of *Streptococcus dysgalactiae* subsp. *dysgalactiae* isolates. The SDSD isolates were stained with 5(6)-Carboxyfluorescein diacetate N-hydroxysuccinimidyl ester (CFSE) fluorophore and propidium iodide, which promotes intracellular labeling of live (green) or dead cells (red); respectively. The left line images were obtained using a green filter (488 nm) and the middle side images were obtained using a red filter (561 nm). Composite image represents the superposition of images acquired for CFSE fluorophore (live cells) and for propidium iodide (dead cells). scale bars with 20 μm. The amplification used was 400 × (For interpretation of the references to colour in this figure legend, the reader is referred to the web version of this article).

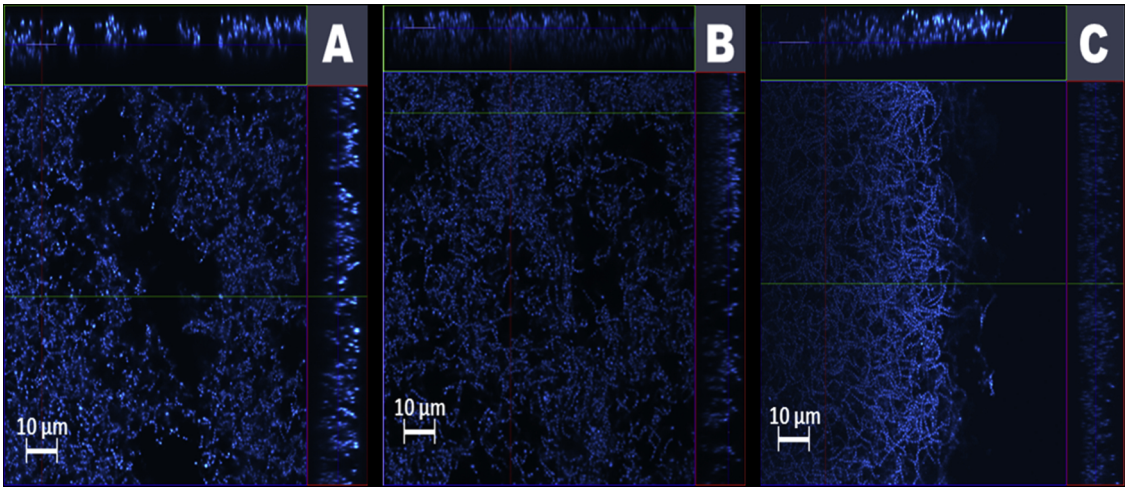

Fig. 3. Confocal fluorescence microscopy of the biofilms produced by *Streptococcus dysgalactiae* subsp. *dysgalactiae* isolates VSD9 (A), VSD10 (B) and VSD16 (C) on glass. Hoechst 33,258 was used to stain the bacterial nucleic acids (blue). The top and right-side rectangular panels are vertical sections representing the XZ plane and YZ plane, respectively, at the positions indicated by the colored line. The biofilms are 9–12 µm, 8–14 µm, 15 µm thick (i.e. Z-axis) respectively. (For interpretation of the references to colour in this figure legend, the reader is referred to the web version of this article).

biofilm, we assessed the *brpA*-like gene in 20 bovine SDSD isolates and in the two Portuguese SDSE strains (HSM53 and COl 289). The genome sequence of SDSE of Lancefield's group A antigen strain AC-2713 (GenBank access number: NC_019042) was used to design overlapping primers for the 1269 bp *brpA*-like gene. The correct amplification product was detected in all SDSD isolates as well as in both control SDSE strains (Supplementary file, S1 table). RT-PCR allowed to demonstrate that the *brpA*-like gene was transcribed in all the tested SDSD and SDSE isolates (Supplementary file, S1 table). The 16S rRNA gene was used as housekeeping gene.

7.7. Real-time qPCR

Transcript levels of *brpA*-like were analysed in the biofilms and in

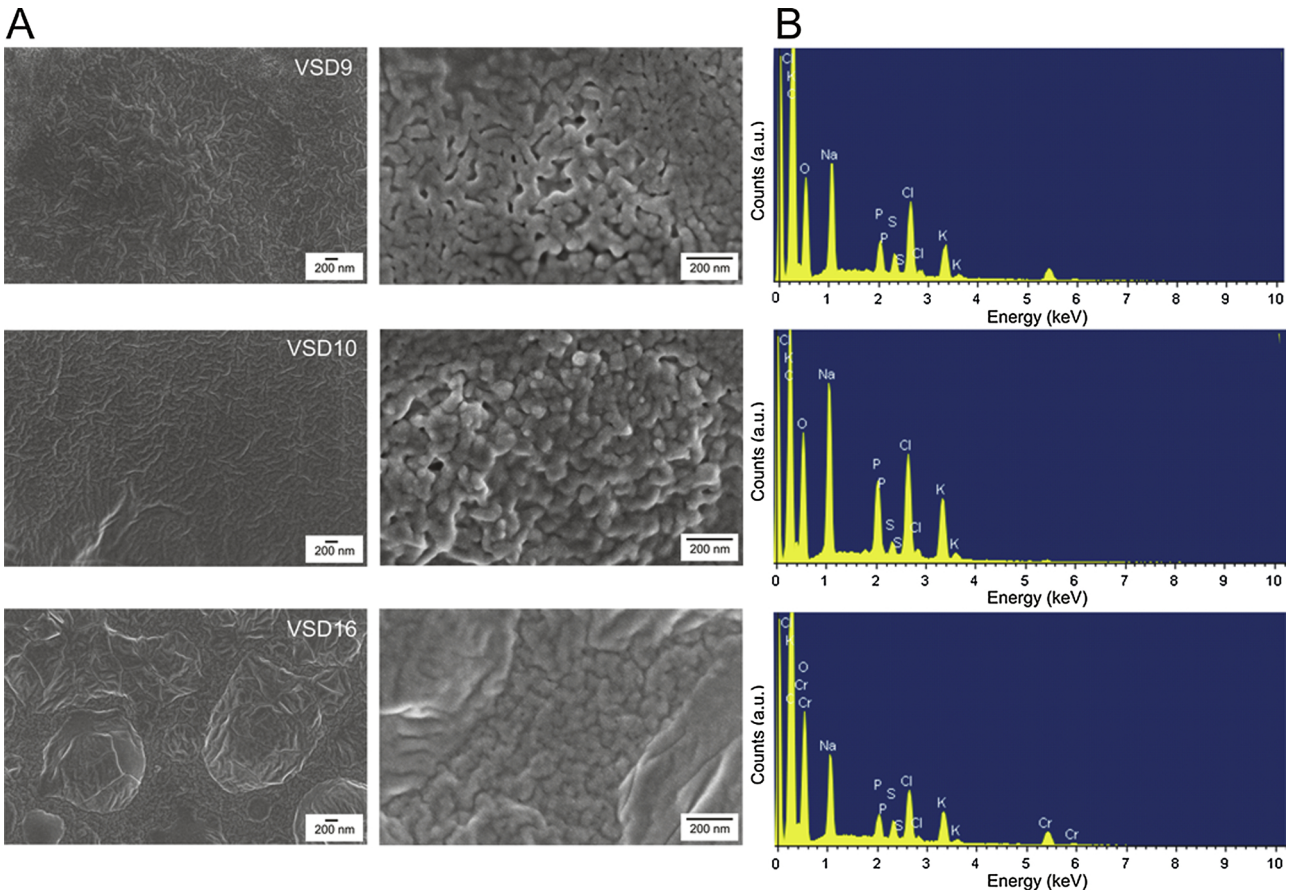

Fig. 4. A) Scanning electron microscopy of *Streptococcus dysgalactiae* subsp. *dysgalactiae* isolates VSD9, VSD10 and VSD16. B) Energy dispersive X-Ray spectroscopy measurements were carried out to compare the elements present at each Biofilm studied.

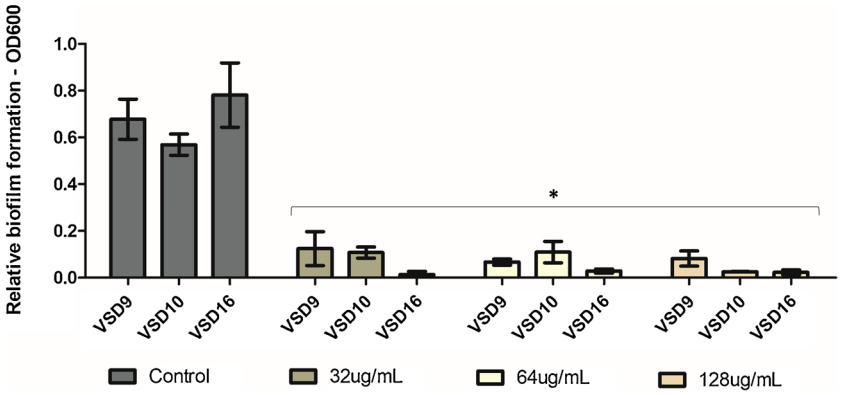

Fig. 5. Inhibition of biofilm formation/accumulation using fisetin, on glass surface by *Streptococcus dysgalactiae* subsp. *dysgalactiae* isolates VSD9, VSD10 and VSD16. Concentration greater than or equal to 32 µg/mL fisetin resulted in a residual biofilm formation in SDSD compared to the control without Fisetin. Represented values are the mean value with SEM. * p-value < 0.001 for results obtained for the inhibition of biofilm formation by SDSD isolates in the presence of fisetin compared to control (without fisetin).

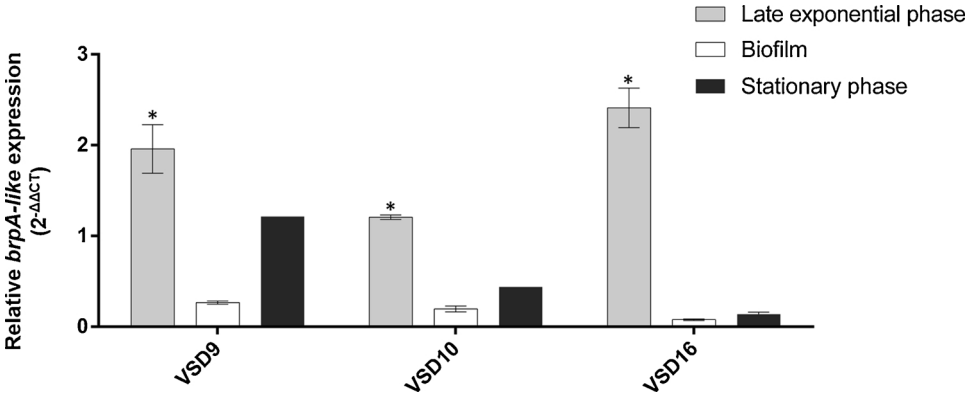

Fig. 6. Expression levels of *brpA*-like in SDSD biofilms (white bars), late exponential phase (grey bars) or stationary phase (black) of planktonic growth. The data are expressed as the means with SEM of three biologically independent experiments. *Statistically significant differences (P < 0.05) between *brpA*-like expression in biofilm relative to the late exponential phase of planktonic growth (For interpretation of the references to colour in this figure legend, the reader is referred to the web version of this article).

the planktonic growth, in the late exponential or stationary phases. This analysis revealed a lower expression of *brpA*-like in biofilm SDSD compared to planktonic in the late exponential phase of growth. The results also showed an increase in the gene expression of VSD9 and VSD16 isolates, during late exponential phase of planktonic growth, when compared to VSD10 isolates. These results are shown in Fig. 6.

7.8. Primary sequence analysis of BrpA homolog protein

SDSD *brpA*-like *gene* was sequenced by primer walking using specific primers and aligned with the *brpA* (*lytR*) homolog from SDSE to get the complete sequence of this gene (Supplementary file, S3 Fig). The *brpA*-like gene sequences of SDSD isolates were submitted to GenBank obtaining the following accession numbers: VSD2 (Accession No. KM485638), VSD6 (KM485639), VSD8 (KM485640), VSD9 (KM485641), VSD15 (KM485642), VSD17 (KM485643), VSD19 (KP308400) and GCS-Mo (KM485644).

BrpA homolog protein of SDSD is a 45,493 Da protein (422 residues) with a computed pI of 5.1. The calculated instability and aliphatic index suggest that it is thermodynamically stable. According to motif search and cell localization prediction, the BrpA-like protein has an *N*-terminal signal peptide (residues 1–27) for cytoplasm secretion, includes a cell envelope-related transcriptional attenuator domain (residues 81–237), with no transmembrane domain. A highly-disordered region is found in the final *ca* 80 residues of the protein (residues 343–422). The detailed results of primary sequence analysis for BrpA homolog protein is given in Supplementary file, S2 Table.

7.9. Predicted structure of BrpA homolog protein and putative inhibitors

The three-dimensional structure of BrpA homolog protein of SDSD is essential for understanding its molecular function and the identification of potential lead molecules for its inhibition. However, a three-dimensional structure of this protein is not yet available, and molecular modeling was used for predicting this structure. The Gbs0355 protein from *Streptococcus agalactiae* (PDB ID: 3OKZ, Northeast Structural Genomics Consortium Target SaR127) has a high sequence identity with BrpA homolog protein (74%) of SDSD and its crystal structure has recently been determined at 2.70 Å resolution. Both Gbs0355 protein and our target protein contain a LytR/CpsA/Psr domain (residues 81–237) and their sequence homology may suggest a common ancestor. Using the ModWeb server (https://modbase.compbio.ucsf.edu/modweb/) (Pieper et al., 2011) and Gbs0355 as a template we predicted the 3-D structure of the 48–342 segment of BrpA homolog protein; the model of the full-length protein could not be attained because the C-terminal region (residues 343 to 422) is highly disordered, with no structural homologs available in the Protein Data Bank (www.rcsb.org). In the obtained model, 99.7% of the residues are in the most favored regions of the Ramachandran plot and the rmsd of the superposition with the template is of 0.287 Å. According to the structural prediction, BrpA homolog protein of SDSD is a globular protein with a *αβα* architecture (Supplementary file, S4 Fig), where the six stranded *β*-pleated sheets that form the core of the domain are surrounded by the alpha helices.

Using the *in silico* predicted model, other proteins were found at the Protein Data Bank (www.rcsb.org) (Berman et al., 2000) having high structural similarity, although with low sequence identity. These proteins were from different Gram-positive bacteria and these homologs are listed in the S3 Table. Secondary structure superpositions show that all proteins share the same structural motif with relatively low rmsd values - maximum rmsd of 2.69 Å for the lowest sequence identity match (27%) (Supplementary file, S3 Table).

To identify putative inhibitors of BrpA homologprotein of SDSD, the three-dimensional model was submitted into DrugDiscovery@TACC web portal (https://drugdiscovery.tacc.utexas.edu/), for a virtual screening using AutoDockVina (Trott and Olson, 2010). The snapshot of secondary and three-dimensional model of BrpA protein homolog of SDSD is shown in Fig. 7.

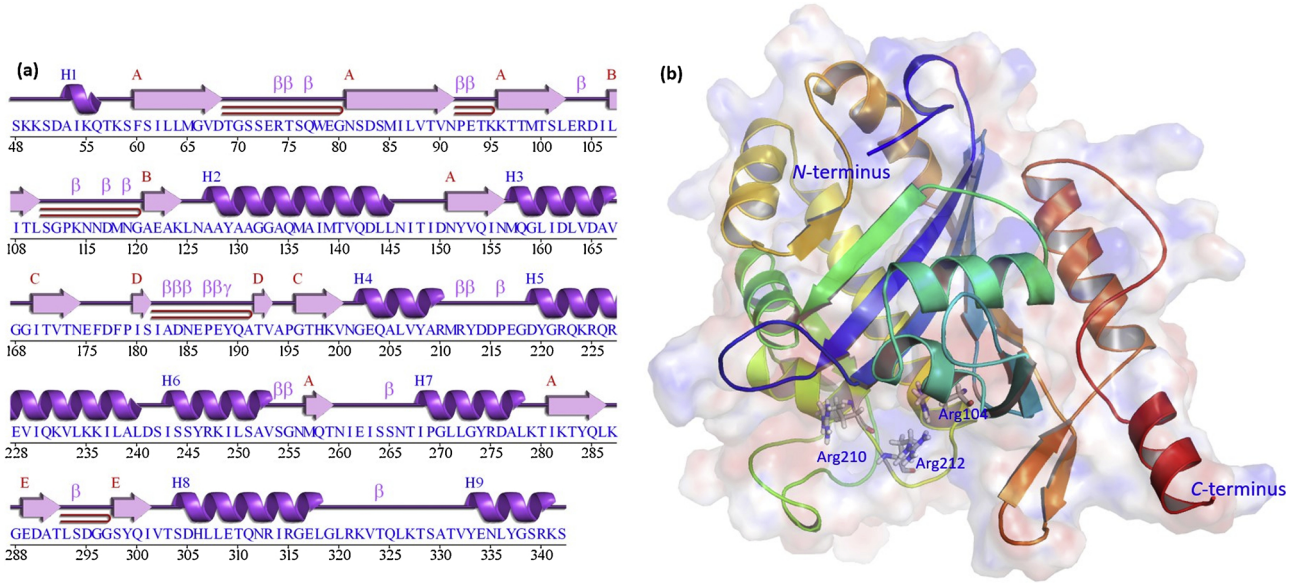

Fig. 7. Snapshot of (A) secondary structure elements and (B) three-dimensional model of BrpA homolog protein and electrostatic potential. The three-dimensional structure was predicted through homology modeling approach. Crucial substrate binding site residues are shown in sticks.

Considering that ellagic acid and fisetin are known biofilm inhibitors, that our data shows that fisetin strongly impairs SDSD biofilm formation, and that *brpA-like* gene is expressed in SDSD, we became interested in knowing if these two inhibitory substances (ellagic acid and Fisetin) could interact with the BrpA homolog of SDSD and used this information to screen additional biofilm inhibitor candidates (Supplementary file, S5 and S6 Figs).

Out of 194,090 screened compounds from the Zinc Natural compound database (http://zinc.docking.org/) (Irwin and Shoichet, 2005), the top five interacting molecules with BrpA protein homolog of SDSD were chosen and thoroughly analyzed (Table 2, Fig. 8). Molecular docking results suggest that all five molecules occupy the same binding pocket in SDSD BrpA homolog protein, interacting with the polypeptide chain via hydrogen bonds and hydrophobic contacts. The high docking scores suggest strong binding affinity (docking results of five putative inhibitors for BrpA homolog protein are shown in Supplementary file, S7–S10 Figs).

In comparison with ellagic acid and fisetin (Table 2, and Supplementary file, S5 Fig and S6 Fig), the proposed five inhibitors show higher binding affinity towards the protein. These highly hydrophobic molecules, rich in aromatic rings, are found in a cleft formed by helices 5 and 7, and, in all five ligand-protein complexes, they are commonly found interacting with Leu64, Leu163, Leu234, Tyr246 amino acid residues. Other hydrophobic residues as Ile62, Leu271 Met257, Ile237, Phe60, Val88, Ile249, Val253, Leu250, and Leu278 are also found to be involved in the same type of interaction, depending on the ligand used for docking. Out of the five molecules, the compound ZINC70704696 is also hydrogen bonded to Tyr246 from an alpha helix at the surface of the protein, putatively stabilizing the ligand in the binding pocket.

8. Discussion

In this study we provide new insights at the molecular level on biofilm development of SDSD. The presented data show for the first time that SDSD isolates accumulate high levels of biofilms on hydrophilic surfaces. The proteinaceous nature of the biofilm matrix was proved by the complete removal of the biologic film after treatment with proteinase. In fact, biofilm production had already been demonstrated in *Streptococcus* spp., including *S. pyogenes* (Young et al., 2016), *S. mutans* (Krzyściak et al., 2014), *S. agalactiae* (Rosini and Margarit, 2015) and *S. dysgalactiae* subsp. *equisimilis* (Genteluci et al., 2015). Additionally, a hydrophilic biofilm matrix, associated to a fimbriae protein, was recently reported for the SDSD-closely related bacteria, SDSE (Genteluci et al., 2015). The implication of biofilm production in the pathogenesis of different infectious diseases, including bovine mastitis has recurrently been reported (Gomes et al., 2016).

The biofilm development by SDSD isolates was also confirmed by fluorescence microscopy, CLSM and SEM. Under SEM observation, the VSD16 isolate formed cell aggregates in the biofilm growth, while VSD9 and VSD10 developed smooth and filmy layers. In addition, a mucous matrix was visualized for VSD16 suggesting differences in biofilm composition for these isolates. The fact that a higher number of dead cells was visualized in VSD16 biofilm indicate increased eDNA content, which is likely to account for the mucous matrix visualized by SEM in the biofilm formed by this SDSD isolate. The importance of eDNA and bacterial proteins:eDNA complexes as components of the biofilm matrixes is well known (Jakubovics et al., 2013). However, our results showed that DNase treatment (in the concentrations used) was not able to disperse the established biofilms. These findings are in agreement with previous studies in which biofilms containing significant quantities of eDNA could not be dispersed by DNase enzymes (Grande et al., 2011; Shields et al., 2013).

Biofilm formation can be considered as a developmental process, which is characterized by a multiple-step structural changes in biofilm architecture and composition, coordinated by a complex net of regulatory genes and environmental signaling via signal transduction (Donlan, 2001; Donlan and Costerton, 2002). Genes associated with intercellular communication systems, sensing systems, carbohydrate metabolism, and adhesion have been described as important and required for the adaptation of *streptococci* in biofilms (Connolly et al., 2011; Marks et al., 2014a, 2014b; Roberts et al., 2010; Wen and Burne, 2002; Senadheera et al., 2005; Shemesh et al., 2007a, 2007b). Among them *brpA (lytR)* encoding BrpA regulatory protein has been described as an important regulator of biofilm formation (Bitoun et al., 2012; Chatfield et al., 2005; Wen et al., 2006; Wen and Burne, 2002). Indeed, in *S. mutans*, the *brpA* gene codes for a predicted surface-associated protein with apparent roles in biofilm formation, autolysis, and cell division. Deficiency of BrpA drastically weakens the ability of the deficient mutant to survive to low pH, oxidative challenge and cell envelope stress (Bitoun et al., 2012; Bitoun et al., 2013). *In vitro*, the BrpA-deficient mutant can bind and establish on a surface, but its ability to accumulate and develop into mature biofilms decreases drastically

Table 2
Potential inhibitors for biofilm regulatory protein, BrpA protein homolog.

Zinc Accession Number	Structure	ΔH (kcal/mol)	Ki (nM)
Known Biofilm inhibitors (Dürig et al., 2010)			
Ellagic acid	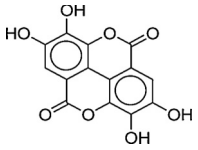	−6.8	10400
Fisetin	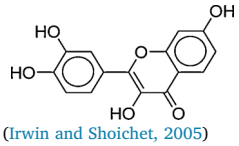	−7.7	2270
Putative inhibitors obtained from Zinc Database (Irwin and Shoichet, 2005)			
ZINC68569433	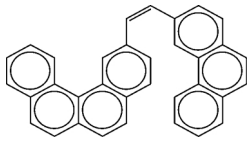	−13.7	0.09
ZINC70704696	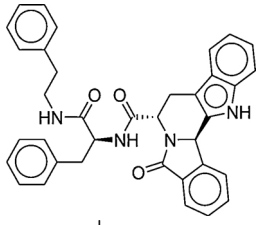	−13.5	0.13
ZINC70705130	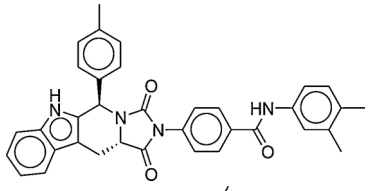	−13.3	0.18
ZINC02666258	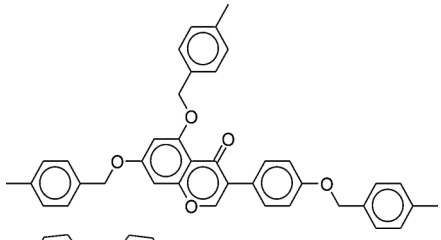	−12.9	0.35
ZINC33906294	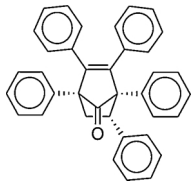	−12.8	0.41

(Bitoun et al., 2012; Bitoun et al., 2013 Wen et al., 2006).

A *brpA*-like gene was detected and able to be transcribed in all the 20 SDSD isolates. The expression of *brpA*-like gene in SDSD biofilms was compared to late exponential and stationary phase of planktonic growth by real-time qPCR. This quantitative analysis revealed lower expression of *brpA*-like in SDSD biofilms compared to late exponential phase of planktonic growth. No significant differences were observed in the expression of *brpA*-like in biofilms compared to stationary phase of planktonic growth. Consistent with the results obtained from biofilm formation on glass, VSD9 and VSD16 isolates showed an increased *brpA*-like expression in the late exponential phase of planktonic growth compared to the VSD10 isolate (Fig. 1 A and 6). Taken together, our data suggest an important role for the BrpA protein in the initial phase of biofilm formation, with a decreased expression in the mature biofilm.

Similar regulation was observed for genes that are involved in the formation of biofilms in *S. pyogenes* (Doern et al., 2009; Reid et al., 2004; Roberts et al., 2010). Due to the inhibition of SDSD biofilm by fisetin, we hypothesized that the inhibitory mechanisms might involve the BrpA homolog. Molecular modeling analysis to predict the 3D structure of BrpA homolog, and a high throughput virtual screening and docking analysis revealed that similarly to fisetin and ellagic acid, the proposed five ligand molecules showed strong binding affinity towards the hydrophobic cleft of the protein. Earlier studies of LCP family proteins suggest that these proteins play a role in the final step of bacterial cell wall synthesis, in particular in the Mg^{2+} dependent phosphotransfer reaction of phospho-teichoic acid and capsular polysaccharides to N-acetyl muramic acid residues of peptidoglycan (Eberhardt et al., 2012; Kawai et al., 2011). Recently, Schaefer et al

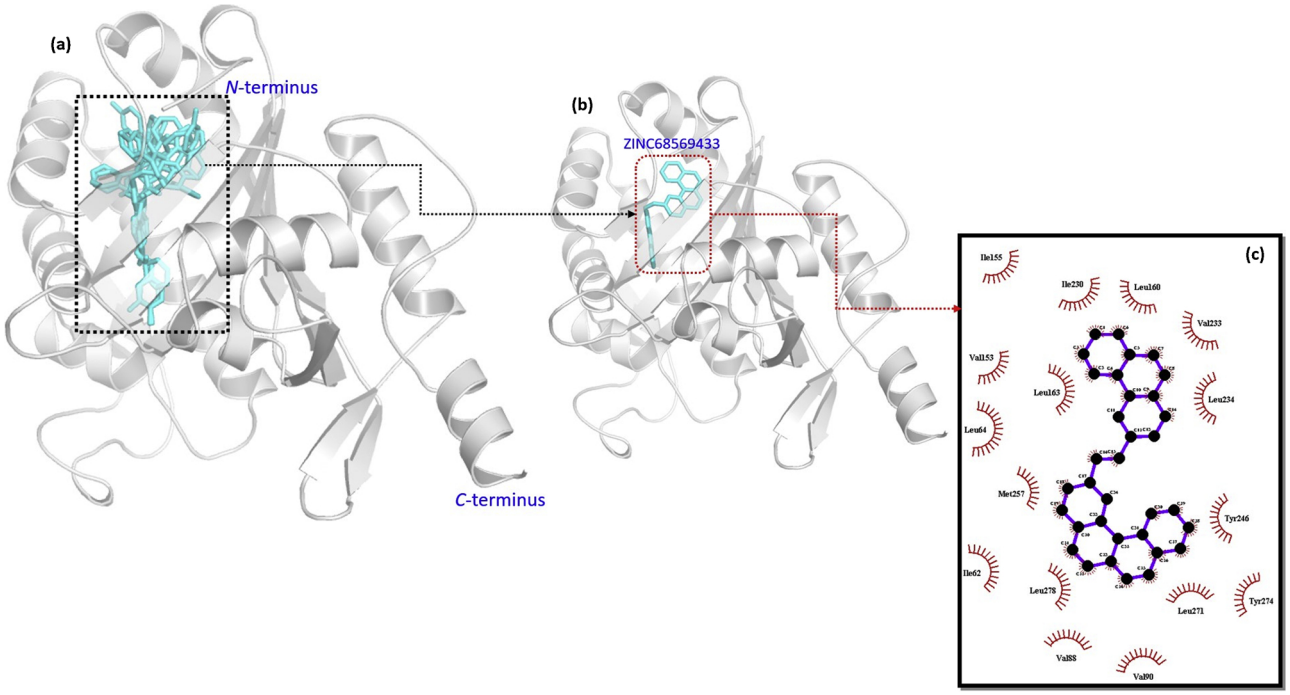

Fig. 8. (a) Orientation of five putative inhibitors (Source: Zinc database) with BrpA protein homolog (b) Binding conformation of first molecule "ZINC68569433" with BrpA protein homolog (c) Two-dimensional ligand interaction diagram of ZINC68569433 with protein (Source-LigPlot). LigPlot shows the amino acid residues of BrpA protein homolog around the putative inhibitor with hydrophobic contacts.

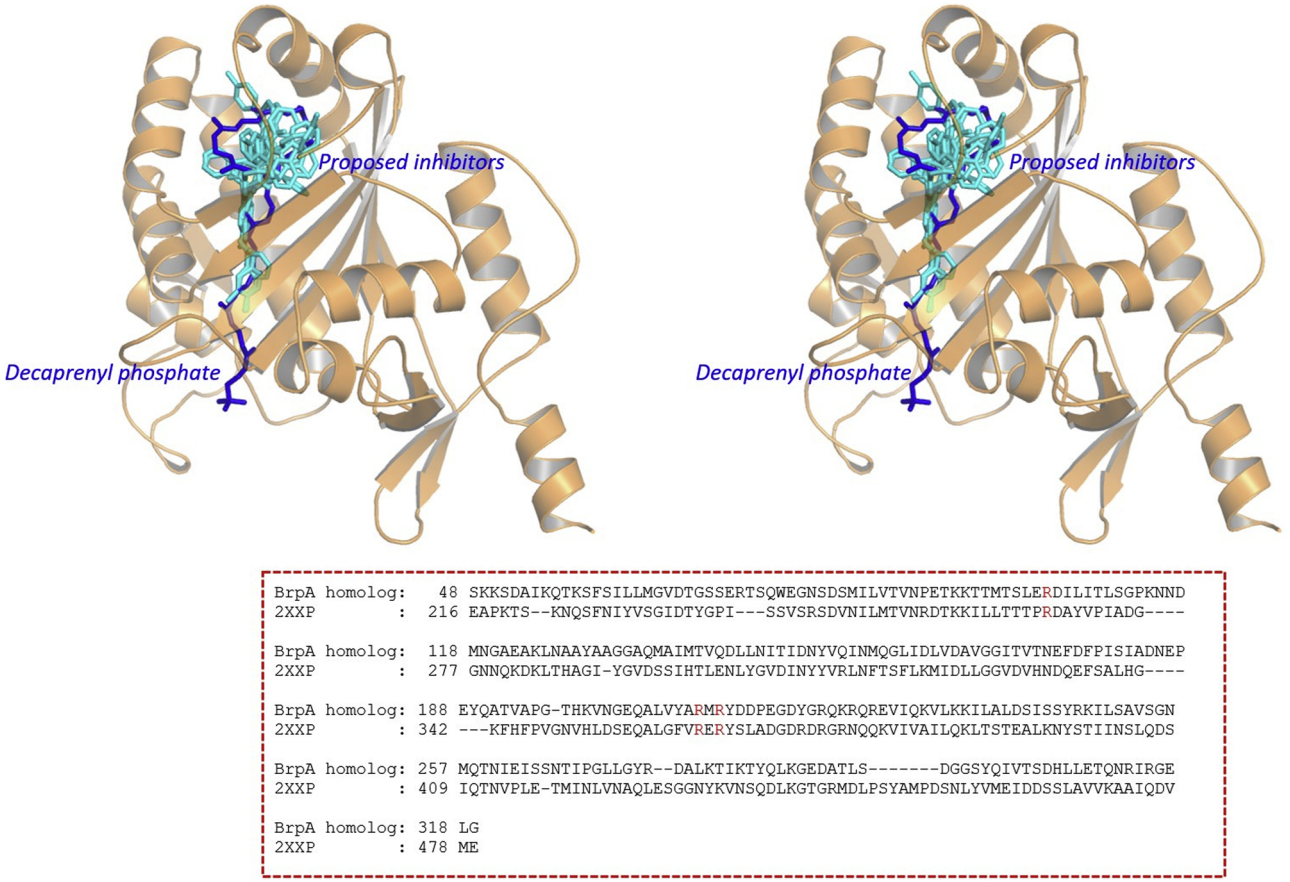

Fig. 9. Stereo view of binding orientation of docking models with crystallographic structure of CPS2A bounded decaprenyl phosphate (PDB ID: 2XXP). Conserved and crucial lipid binding residues are shown in red color (For interpretation of the references to colour in this figure legend, the reader is referred to the web version of this article).

showed that, in *S. aureus*, the homolog protein LcpA is responsible for ligating peptidoglycan oligomers to wall teichoic acids via a phosphodiester bond (Schaefer et al., 2017). The crystal structures of *Streptococcus pneumoniae* D39 and *Bacilus subtilis* homolog proteins have been solved in a complex with phospholipids which were found at the active site, in a hydrophobic cleft. Superposition of these structures with our docking results show that the putative inhibitors are occupying the phospholipid binding site (Fig. 9, Supplementary file, S11 Fig) (PDB Ids: 2XXP, 2XXQ, 3TEL, 3TEP, 3 TF L, 4DE8 and 4DE9). Moreover, a detailed analysis of the models indicates that the residues important for lipid binding are also present in the SDSD BrpA homolog protein, namely the highly-conserved arginine's at the surface of the protein, and the aspartate residues that bind Mg^{2+} ions. In addition, the following lipid binding site residues are also conserved in both proteins as depicted in Fig. 9. Both types of interaction have been suggested to be crucial for protein activity and peptidoglycan formation. To better understand and characterize BrpA homolog protein, site directed mutagenesis and x-ray protein crystallography assays are under way.

It is interesting that, in this study, fisetin dramatically inhibited biofilm formation of SDSD isolates, but at the tested concentrations did not affect planktonic growth. Similar results were previously reported for *Staphylococcus aureus* and *Streptococcus dysgalactiae* (Dürig et al., 2010). Taking all together, our data might indicate that inhibition of biofilm formation in SDSD may be mediated by interactions between fisetin and BrpA protein homolog, and this protein might be an important target for the molecular design of antibiofilm drugs. However, further studies should be performed to directly confirm these interactions.

9. Conclusion

Our study shows for the first time that SDSD can grow forming a biofilm environment, which may be an important factor in the pathogenesis of mastitis. In addition, we show that *brpA*-like gene is present and expressed in SDSD biofilm-producing isolates, and that fisetin dramatically inhibited biofilm formation of SDSD isolates but at the tested concentrations did not affect planktonic growth. Taken together, our data suggest an important role for the *brpA*-like gene in biofilm formation. Finally, homology modelling and docking analysis selected potential lead inhibitors candidates of BrpA protein homolog. However, further investigations are necessary to better understand the role of BrpA homolog in the regulation of biofilm associated genes.

Acknowledgements

This work was supported by the Unidade de Ciências Biomoleculares Aplicadas-UCIBIO which is financed by national funds from FCT/MEC (UID/Multi/04378/2013) and also by projects PTDC/CVT-EPI/4651/2012 and PTDC/CVT-EPI/6685/2014. FCT-MEC is also acknowledged the grant SFRH/BD/118350/2016 to CAB and SFRH/BPD/97719/2013 to JM. The authors thank M. Costa for preliminary SEM assessment. None of the authors have any potential conflicts of interest.

Appendix A. Supplementary data

Supplementary material related to this article can be found, in the online version, at doi:https://doi.org/10.1016/j.ijmm.2019.02.001.

References

Alves-Barroco, C., Roma-Rodrigues, C., Raposo, L.R., et al., 2018. *Streptococcus dysgalactiae subsp. dysgalactiae* isolated from milk of the bovine udder as emerging pathogens: in vitro and in vivo infection of human cells and zebrafish as biological models. MicrobiologyOpen (January), 1–13. https://doi.org/10.1002/mbo3.623.

Berman, H.M., Westbrook, J., Feng, Z., et al., 2000. The protein data bank. Nucleic Acids Res. 28 (1), 235–242. https://doi.org/10.1093/nar/28.1.235.

Bitoun, J.P., Liao, S., Yao, X., Ahn, Sj., Isoda, R., Nguyen, A.H., Brady, L.J., Burne, R.A., Abranches, J., Wen, Z.T., 2012. BrpA is involved in regulation of cell envelope stress responses in *Streptococcus mutans*. Appl. Environ. Microbiol. 78 (8), 2914–2922. https://doi.org/10.1128/AEM.07823-11.

Bitoun, J.P., Liao, S., McKey, B.A., Yao, X., Fan, Y., Abranches, J., Beatty, W.L., Wen, Z.T., 2013. Psr is involved in regulation of glucan production, and double deficiency of BrpA and Psr is lethal in *Streptococcus mutans*. Microbiology 159 (Mar (Pt 3)), 493–506. https://doi.org/10.1099/mic.0.063032-0. Epub 2013 Jan 3.

Bitoun, J.P., Liao, S., Xie, G.G., Beatty, W.L., Wen, Z.T., 2014. Deficiency of BrpB causes major defects in cell division, stress responses and biofilm formation by *Streptococcus mutans*. Microbiol (United Kingdom). 160, 67–78. https://doi.org/10.1099/mic.0.072884-0.

Camacho, C., Coulouris, G., Avagyan, V., et al., 2009. BLAST+: architecture and applications. BMC Bioinform. 10. https://doi.org/10.1186/1471-2105-10-421.

Chatfield, C.H., Koo, H., Quivey, R.G., 2005. The putative autolysin regulator LytR in *Streptococcus mutans* plays a role in cell division and is growth-phase regulated. Microbiology 151 (2), 625–631. https://doi.org/10.1099/mic.0.27604-0.

Connolly, K.L., Roberts, A.L., Holder, R.C., Reid, S.D., 2011. Dispersal of group a streptococcal biofilms by the cysteine protease *SpeB* leads to increased disease severity in a murine model. PLoS One 6 (April (4)), e18984. https://doi.org/10.1371/journal.pone.0018984.

Crang, R.F.E., Klomparens, K.L., 1988. Artifacts in biological electron microscopy. Science 242 (4876), 309. https://doi.org/10.1126/science.242.4876.309.

Del Pozo, J.L., 2018. Biofilm-related disease. Expert Rev. Anti-Infect. Ther. 16 (1), 51–65. https://doi.org/10.1080/14787210.2018.1417036.

Doern, C.D., Roberts, A.L., Hong, W., Nelson, J., Lukomski, S., Swords, W.E., Sean, Reid, 2009. Biofilm formation by group A Streptococcus: a role for the streptococcal regulator of virulence (Srv) and streptococcal cysteine protease (SpeB). Microbiology 155 (Pt 1), 46–52. https://doi.org/10.1099/mic.0.021048-0.

Donlan, R.M., 2001. Biofilm formation: a clinically relevant microbiological process. Clin. Infect. Dis. 33 (8), 1387–1392. https://doi.org/10.1086/322972.

Donlan, R.M., Costerton, J.W., 2002. Biofilms survival mechanisms of clinically relevant microorganisms. Clin. Microbiol. Rev. 15 (April (2)), 167–193. https://doi.org/10.1128/CMR.15.2.167-193.2002.

Dürig, A., Kouskoumvekaki, I., Vejborg, R.M., Klemm, P., 2010. Chemoinformatics-assisted development of new anti-biofilm compounds. Appl. Microbiol. Biotechnol. 87 (1), 309–317. https://doi.org/10.1007/s00253-010-2471-0.

Dykstra, M.J., Reuss, L.E., 2003. Biological Electron Microscopy. Kluwer Academic/Plenum Publishers, New York. https://doi.org/10.1007/978-1-4419-9244-4.

Eberhardt, A., Hoyland, C.N., Vollmer, D., et al., 2012. Attachment of capsular polysaccharide to the cell wall in Streptococcus pneumoniae. Microb. Drug Resist. 18 (3), 240–255. https://doi.org/10.1089/mdr.2011.0232.

Ferreira, F.A., Souza, R.R., Bonelli, R.R., Américo, M.A., Fracalanzza, S.E.L., Figueiredo, A.M.S., 2012. Comparison of in vitro and in vivo systems to study ica-independent *Staphylococcus aureus* biofilms. J. Microbiol. Methods 88 (3), 393–398. https://doi.org/10.1016/j.mimet.2012.01.007.

Flemming, H.C., Wingender, J., 2010. The biofilm matrix. Nat. Rev. Microbiol. 8 (9), 623–633. https://doi.org/10.1038/nrmicro2415.

Galante, J., Ho, A.C.Y., Tingey, S., Charalambous, B.M., 2015. Quorum sensing and biofilms in the pathogen, *Streptococcus pneumoniae*. Curr. Pharm. Des. 21 (1), 25–30. http://www.ncbi.nlm.nih.gov/pubmed/25189864.

Gardy, J.L., Spencer, C., Wang, K., et al., 2003. PSORT-B: improving protein subcellular localization prediction for gram-negative bacteria. Nucleic Acids Res. 31 (13), 3613–3617. https://doi.org/10.1093/nar/gkg602.

Garnett, J.A., Matthews, S., 2012. Interactions in bacterial biofilm development: a structural perspective. Curr. Protein Pept. Sci. 13 (8), 739–755. https://doi.org/10.2174/138920312804871166.

Gasteiger, E., Hoogland, C., Gattiker, A., et al., 2005. Protein identification and analysis tools on the ExPASy server. Proteomics Protoc. Handb. 571–607. https://doi.org/10.1385/1-59259-890-0:571.

Genteluci, G.L., Silva, L.G., Souza, M.C., et al., 2015. Assessment and characterization of biofilm formation among human isolates of *Streptococcus dysgalactiae* subsp. *equisimilis*. Int. J. Med. Microbiol. 305 (8), 937–947. https://doi.org/10.1016/j.ijmm.2015.10.004.

Ghinet, M.G., Asli, A., Brouillette, E., Brzezinski, R., Lacasse, P., Jacques, M., 2017. Antibiofilm and Antibacterial Effects of Specific Chitosan Molecules on *Staphylococcus aureus* Isolates Associated With Bovine Mastitis. pp. 23. https://doi.org/10.1371/journal.pone.0176988.

Gomes, L.C., Mergulhão, F.J., 2017. SEM analysis of surface impact on biofilm antibiotic treatment. Scanning. https://doi.org/10.1155/2017/2960194.

Gomes, F., Saavedra, M.J., Henriques, M., 2016. Bovine mastitis disease/pathogenicity: evidence of the potential role of microbial biofilms. Pathog. Dis. 74 (3), 1–7. https://doi.org/10.1093/femspd/ftw006.

Grande, R., Di Giulio, M., Bessa, L.J., et al., 2011. Extracellular DNA in *Helicobacter pylori* biofilm: a backstairs rumour. J. Appl. Microbiol. 1 (2), 490–498. https://doi.org/10.1111/j.1365-2672.2010.04911.x. 10.

Irwin, J.J., Shoichet, B.K., 2005. ZINC - a free database of commercially available compounds for virtual screening. J. Chem. Inf. Model. 45 (1), 177–182. https://doi.org/10.1021/ci049714+.

Jakubovics, N.S., Shields, R.C., Rajarajan, N., Burgess, J.G., 2013. Life after death: the critical role of extracellular DNA in microbial biofilms. Lett. Appl. Microbiol. 57 (6), 467–475. https://doi.org/10.1111/lam.12134.

Jefferson, K.K., 2004. What drives bacteria to produce a biofilm? FEMS Microbiol. Lett. 236 (2), 163–173. https://doi.org/10.1016/j.femsle.2004.06.005.

Jordal, S., Glambek, M., Oppegaard, O., Kittang, B.R., 2015. New tricks from an old cow: infective endocarditis caused by *Streptococcus dysgalactiae* subsp. *dysgalactiae*. J. Clin.

Microbiol. 53 (2), 731–734. https://doi.org/10.1128/JCM.02437-14.
Kawai, Y., Marles-Wright, J., Cleverley, R.M., et al., 2011. A widespread family of bacterial cell wall assembly proteins. EMBO J. 30 (24), 4931–4941. https://doi.org/10.1038/emboj.2011.358.
Koh, T.H., Sng, L.H., Yuen, S.M., et al., 2009. Streptococcal cellulitis following preparation of fresh raw seafood. Zoonoses Public Health 56 (4), 206–208. https://doi.org/10.1111/j.1863-2378.2008.01213.x.
Kostakioti, M., Hadjifrangiskou, M., Hultgren, S.J., 2013. Bacterial biofilms: development, dispersal, and therapeutic strategies in the dawn of the postantibiotic era. Cold Spring Harb. Perspect. Med. 3 (4), 1–23. https://doi.org/10.1101/cshperspect.a010306.
Krzyściak, W., Jurczak, A., Kościelniak, D., Bystrowska, B., Skalniak, A., 2014. The virulence of *Streptococcus mutans* and the ability to form biofilms. Eur. J. Clin. Microbiol. Infect. Dis. 33 (4), 499–515. https://doi.org/10.1007/s10096-013-1993-7.
Kvist, M., Hancock, V., Klemm, P., 2008. Inactivation of efflux pumps abolishes bacterial biofilm formation. Appl. Environ. Microbiol. 74 (23), 7376–7382. https://doi.org/10.1128/AEM.01310-08.
Laskowski, R.A., Swindells, M.B., 2011. LigPlot+: multiple ligand-protein interaction diagrams for drug discovery. J. Chem. Inf. Model. 51 (10), 2778–2786. https://doi.org/10.1021/ci200227u.
Lee, S.F., Delaney, G.D., Elkhateeb, M., 2004. A two-component covRS regulatory system regulates expression of fructosyltransferase and a novel extracellular carbohydrate in *Streptococcus mutans*. Infect. Immun. 72 (7), 3968–3973. https://doi.org/10.1128/IAI.72.7.3968-3973.2004.
Li, Y., Burne, R.A., 2001. Regulation of the gtfBC and ftf genes of *Streptococcus mutans* in biofilms in response to pH and carbohydrate. Microbiology 147 (10), 2841–2848. https://doi.org/10.1099/00221287-147-10-2841.
Lovell, S.C., Davis, I.W., Adrendall, W.B., et al., 2003. Structure validation by C alpha geometry: phi,psi and C beta deviation. Proteins-Struct. Funct. Genet. 50 (August 2002), 437–450. https://doi.org/10.1002/prot.10286.
Marks, L.R., Reddinger, R.M., Hakansson, A.P., 2014a. Biofilm formation enhances fomite survival of *Streptococcus pneumoniae* and *Streptococcus pyogenes*. Infect. Immun. 82 (3), 1141–1146. https://doi.org/10.1128/IAI.01310-13.
Marks, L.R., Mashburn-Warren, L., Federle, M.J., Hakansson, A.P., 2014b. *Streptococcus pyogenes* biofilm growth in vitro and in vivo and its role in colonization, virulence, and genetic exchange. J. Infect. Dis. 210 (1), 25–34. https://doi.org/10.1093/infdis/jiu058.
Oliver-Kozup, H.A., Elliott, M., Bachert, B.A., et al., 2011. The streptococcal collagen-like protein-1 (Scl1) is a significant determinant for biofilm formation by group A Streptococcus. BMC Microbiol. 11 (1), 262. https://doi.org/10.1186/1471-2180-11-262.
Olsen, I., 2015. Biofilm-specific antibiotic tolerance and resistance. Eur. J. Clin. Microbiol. Infect. Dis. 34 (5), 877–886. https://doi.org/10.1007/s10096-015-2323-z.
Park, M.J., Eun, I.S., Jung, C.Y., et al., 2012. *Streptococcus dysgalactiae* subspecies dysgalactiae infection after total knee arthroplasty: a case report. Knee Surg. Relat. Res. 24 (2), 120–123. https://doi.org/10.5792/ksrr.2012.24.2.120.
Parnasa, R., Nagar, E., Sendersky, E., Reich, Ziv., Simkovsky, R., Golden, S., Schwarz, R., 2016. Small secreted proteins enable biofilm development in the cyanobacterium *Synechococcus elongatus*. Sci. Rep. 1–10. https://doi.org/10.1038/srep32209.
Pieper, U., Webb, B.M., Barkan, D.T., et al., 2011. ModBase, a database of annotated comparative protein structure models, and associated resources. Nucleic Acids Res. 39 (Suppl. 1), 465–474. https://doi.org/10.1093/nar/gkq1091.
Pluk, H., Stokes, D.J., Lich, B., Wieringa, B., Fransen, J., 2009. Advantages of indium tin oxide coated glass slides in correlative scanning electron microscopy applications of uncoated cultured cells. J. Microsc. 233 (3), 353–363. https://doi.org/10.1111/j.1365-2818.2009.03140.x.
Rato, M.G., Bexiga, R., Nunes, S.F., Vilela, C.L., Santos-Sanches, I., 2010. Human group A streptococci virulence genes in bovine group C streptococci. Emerg. Infect. Dis. 16 (1), 116–119. https://doi.org/10.3201/eid1601.090632.
Rato, M.G., Nerlich, A., Bergmann, R., et al., 2011. Virulence gene pool detected in bovine group C *Streptococcus dysgalactiae subsp. dysgalactiae* isolates by use of a group A S. pyogenes virulence microarray. J. Clin. Microbiol. 49 (7), 2470–2479. https://doi.org/10.1128/JCM.00008-11.
Reid, S.D., Montgomery, A.G., Musser, J.M., 2004. Identification of Srv, a PrfA-like regulator of group A Streptococcus that influences virulence. Infect. Immun. 72 (3), 1799–1803.
Reid, S.D., Hong, W., Dew, K.E., et al., 2009. *Streptococcus pneumoniae* forms surface-attached communities in the middle ear of experimentally infected chinchillas. J. Infect. Dis. 199 (6), 786–794. https://doi.org/10.1086/597042.
Roberts, A.L., Connolly, K.L., Doern, C.D., Holder, R.C., Reid, S.D., 2010. Loss of the group a Streptococcus regulator srv decreases biofilm formation *in vivo* in an otitis media model of infection. Infect. Immun. 4800–4808. https://doi.org/10.1128/IAI.00255-10.
Rollefson, J.B., Stephen, C.S., Tien, M., Bond, D.R., 2011. Identification of an extracellular polysaccharide network essential for cytochrome anchoring and biofilm formation in *Geobacter sulfurreducens*. J. Bacteriol. 193 (5), 1023–1033. https://doi.org/10.1128/JB.01092-10.
Roma-Rodrigues, C., Alves-Barroco, C., Raposo, L.R., et al., 2015. Infection of human keratinocytes by *Streptococcus dysgalactiae subspecies dysgalactiae* isolated from milk of the bovine udder. Microbes Infect. https://doi.org/10.1016/j.micinf.2015.11.005.
Rosini, R., Margarit, I., 2015. Biofilm formation by *Streptococcus agalactiae*: influence of environmental conditions and implicated virulence factors. Front. Cell. Infect. Microbiol. 5 (February), 2013–2016. https://doi.org/10.3389/fcimb.2015.00006.
Rother, K., 2005. Introduction to PyMOL. Methods Mol Biol Clift Nj. 635 (8), 0–32. https://doi.org/10.1213/ANE.0b013e3181e9c3f3.
Savage, V.J., Chopra, I., O'Neill, A.J., 2013. *Staphylococcus aureus* biofilms promote horizontal transfer of antibiotic resistance. Antimicrob. Agents Chemother. 57 (4), 1968–1970. https://doi.org/10.1128/AAC.02008-12.
Schaefer, K., Matano, L.M., Qiao, Y., Kahne, D., Walker, S., 2017. *In vitro* reconstitution demonstrates the cell wall ligase activity of LCP proteins. Nat. Chem. Biol. 13 (4), 396–401. https://doi.org/10.1038/nchembio.2302.
Senadheera, M.D., Guggenheim, B., Spatafora, G.A., Huang, Y.C., Choi, J., Hung, D.C., Treglown, J.S., Goodman, S.D., Ellen, R.P., Cvitkovitch, D.G., 2005. A VicRK signal transduction system in *Streptococcus mutans* affects gtfBCD, gbpB, and ftf expression, biofilm formation, and genetic competence development. J. Bacteriol. 187, 4064–4076. https://doi.org/10.1128/JB.187.12.4064-4076.2005.
Seppalla, H., Skurnik, M., Soini, H., Roberts, M.C., Huovinen, P., 1998. A novel erythromycin resistance methylase gene (ermTR) in *Streptococcus pyogenes*. Antimicrob. Agents Chemother. 42 (2), 257–262.
Shemesh, M., Tam, A., Steinberg, D., 2007a. Differential gene expression profiling of *Streptococus mutans* cultured under biofilm and planktonic conditions. Microbiology 153 (5), 1307–1317. https://doi.org/10.1099/mic.0.2006/002030-0.
Shemesh, M., Tam, A., Steinberg, D., 2007b. Expression of biofilm-associated genes of *Streptococcus mutans* in response to glucose and sucrose. J. Med. Microbiol. 153 (5), 1528–1535. https://doi.org/10.1099/jmm.0.47146-0. 56(11).
Shields, R.C., Mokhtar, N., Ford, M., et al., 2013. Efficacy of a marine bacterial nuclease against biofilm forming microorganisms isolated from chronic rhinosinusitis. PLoS One 8 (2). https://doi.org/10.1371/journal.pone.0055339.
Silva, V.O., Soares, L.O., Chang, Y., Moreira, M.A.S., 2014. Biofilm formation on biotic and abiotic surfaces in the presence of antimicrobials by *Escherichia coli* isolates from cases of bovine mastitis. Appl. Environ. Microbiol. 80 (19), 6136–6145. https://doi.org/10.1128/AEM.01953-14.
Stepanović, S., Vuković, D., Hola, V., Di Bonaventura, G., Djukić, S., Cirković, I., Ruzicka, F., 2007. Quantification of biofilm in microtiter plates: overview of testing conditions and practical recommendations for assessment of biofilm production by staphylococci. APMIS 115, 891–899. https://doi.org/10.1111/j.1600-0463.2007.apm_630.x.
Toledo-arana, A., Merino, N., Débarbouillé, M., et al., 2005. *Staphylococcus aureus* develops an alternative, ica- independent biofilm in the absence of the arlRS two-component system *Staphylococcus aureus* develops an alternative, ica- independent biofilm in the absence of the arlRS two-component system. J. Bacteriol. 187 (15), 5318–5329. https://doi.org/10.1128/JB.187.15.5318.
Trott, O., Olson, A., 2010. AutoDock Vina: improving the speed and accuracy of docking with a new scoring function, efficient optimization and multithreading. J. Comput. Chem. 31 (2), 455–461. https://doi.org/10.1002/jcc.21334.
Tsirigos, K.D., Peters, C., Shu, N., Käll, L., Elofsson, A., 2015. The TOPCONS web server for consensus prediction of membrane protein topology and signal peptides. Nucleic Acids Res. 43 (W1), W401–W407. https://doi.org/10.1093/nar/gkv485.
Wen, Z.T., Burne, R.A., 2002. Functional genomics approach to identifying genes required for biofilm development by *Streptococcus mutans*. Appl. Environ. Microbiol. 68 (3), 1196–1203. https://doi.org/10.1128/AEM.68.3.1196.
Wen, Z.T., Baker, H.V., Burne, R.A., 2006. Influence of BrpA on critical virulence attributes of *Streptococcus mutans*. Appl. Environ. Microbiol. 188 (8), 2983–2992. https://doi.org/10.1128/JB.188.8.2983-2992.2006.
Young, C., Holder, R.C., Dubois, L., Reid, S.D., 2016. *Streptococcus pyogenes* Biofilm. pp. 1–26.